Aberystwyth University

Determining leaf area index and leafy tree roughness using terrestrial laser scanning
Muller, E.; Antonarakis, A. S.; Brasington, James; Richards, Keith S.

Determining leaf area index and leafy tree roughness using terrestrial laser scanning

A. S. Antonarakis,[1] K. S. Richards,[2] J. Brasington,[3] and E. Muller[4]

[1] Vegetation roughness, and more specifically forest roughness, is a necessary component in better defining flood dynamics both in the sense of changes in river catchment characteristics and the dynamics of forest changes and management. Extracting roughness parameters from riparian forests can be a complicated process involving different components for different required scales and flow depths. For flow depths that enter a forest canopy, roughness at both the woody branch and foliage level is necessary. This study attempts to extract roughness for this leafy component using a relatively new remote sensing technique in the form of terrestrial laser scanning. Terrestrial laser scanning is used in this study due to its ability to obtain millions of points within relatively small forest stands. This form of lidar can be used to determine the gaps present in foliaged canopies in order to determine the leaf area index. The leaf area index can then be directly input into resistance equations to determine the flow resistance at different flow depths. Leaf area indices created using ground scanning are compared in this study to indices calculated using simple regression equations. The dominant riparian forests investigated in this study are planted and natural poplar forests over a lowland section of the Garonne River in Southern France. Final foliage roughness values were added to woody branch roughness from a previous study, resulting in total planted riparian forest roughness values of around Manning's $n = 0.170–0.195$ and around $n = 0.245–330$ for in-canopy flow of 6 and 8 m, respectively, and around $n = 0.590$ and around $n = 0.750$ for a natural forest stand at the same flow depths.

1. Introduction

[2] Deriving vegetation roughness for forests with different structural characteristics is a necessary component in resistance calculations and flood modeling exercises. Lidar has to potential to extract 3-D structural information for forests. Airborne lidar has previously been used to extract trunk roughness for below canopy flow [*Antonarakis et al.*, 2008]. Terrestrial or ground lidar has the capability to recover more detailed structural information from forest canopies. Terrestrial lidar has been used in a previous study to determine the roughness of complex leafless tree canopies [*Antonarakis et al.*, 2009].

[3] A more complete consideration of the roughness of complex tree canopies involves the leafy component of a canopy as well as its bare branches. The calculation of vegetation roughness allowing for tall trees in a riparian zone has not been considered adequately in research. It has been sug-gested that one of the fundamental properties of resistance through vegetation is the density of the vegetation and the deformation of the plant in flow [*Fathi-Moghadam and Kouwen*, 1997; *Kouwen and Li*, 1980]. The density and deformation of the leafy component of a tree can be a major contributor to the overall vegetation roughness. The leafy component could then be used in resistance equations, where the projected leaf area can be compared to its density and size by relating it to the horizontal area it occupies. This is called the leaf area index (LAI) and is defined as the projected green (living) leaf area per unit surface area of the ground in broadleaf canopies [*Curran and Williamson*, 1987]. It is also defined as the total leaf surface area exposed to incoming light or radar energy, expressed in relation to the ground surface area beneath the plant. *Järvelä* [2004] has considered the roughness of leafy vegetation, incorporating aspects such as the LAI and other vegetation parameters. Instead of using flexibility parameters such as the nonsubmerged vegetation factor (ξE) defined by *Fathi-Moghadam and Kouwen* [1997], *Järvelä* [2004] has incorporated species-specific parameters such as the vegetation resonance parameter (χ) and the species-specific drag coefficient ($C_{d\chi}$).

[4] The LAI is the major factor determining the amount of energy that is intercepted by the plant canopy, but it varies greatly with species and canopy structure. Recent techniques for determining the leaf area index have focused on the use of digital sensors that are placed in the forested sections and can automatically gain information on the LAI of that stand. For example, these techniques include instruments

[1]Department of Organismic and Evolutionary Biology, Harvard University, Cambridge, Massachusetts, USA.
[2]Department of Geography, University of Cambridge, Cambridge, UK.
[3]Institute of Geography and Earth Sciences, University of Wales, Aberystwyth, UK.
[4]Laboratoire Dynamique de la Biodiversité, CNRS, Toulouse, France.

such as the CI-100 Digital Plant Canopy Imager [e.g., *Peper and McPherson*, 2003; *Jonckheere et al.*, 2004] and the LAI-2000 Plant Canopy Analyzer [e.g., *Deblonde et al.*, 1994; *Cutini et al.*, 1998] focusing on the canopy gaps and intensity of light transmitted through a canopy. Airborne lidar cannot provide any explicit information of the leafy structure of a canopy, so studies focusing on determining LAI from airborne lidar have regressed other structural attributes to leaf area [e.g., *Roberts et al.*, 2005; *Farid et al.*, 2009]. Few studies have attempted gap fraction or leaf area measurements from terrestrial lidar. *Clawges et al.* [2007] used a terrestrial scanner to estimate the leaf area of the pine species *Larix occidentalis*, by regressing the needle-leaf millimeter returns with the known leaf areas. *Danson et al.* [2007] developed a method that considered the points returned and lost from a ground lidar directed at a tree canopy was equivalent to the traditional transmission or gap fraction used by leaf area studies such as that given by *Norman and Campbell* [1989] and was likened to LAIs determined from hemispherical photography. Ground lidar gap fractions were successfully compared to hemispherical photography in the study by *Lovell et al.* [2003]. LAI calculations have recently been achieved with new waveform-digitizing ground lidar [*Strahler et al.*, 2008].

[5] The aim of this study was to determine the leafy roughness of complex woody vegetation using the relatively new and powerful terrestrial-based laser scanning (TLS) remote sensing technique, in order to parameterize roughness of the leafy component of trees. A method is presented in this paper that derives the LAI and subsequently the leafy roughness of various forest stands using terrestrial laser scanning. Here directional gap fractions of the various forests will first be determined using detailed ground scans of the leafy stands comparable to work done by *Danson et al.* [2007]. Then, this information will be applied to the well-known Beer-Lambert transmittance law [*Nel and Wessman*, 1993], to determine the leaf area index in a forest type. These leaf area indices determined for the study sites will be compared to the LAI measured in the field from a mature planted poplar of the Garonne. The leaf area indices will also be compared to a standard allometric relationship defined by *Niklas* [1994] and species-specific regression relationships defined by *Gielen et al.* [2001] relating the leaf area to trunk diameters.

[6] The next sections briefly describe field sites where ground scanning data were collected, and subsequently, the resistance equation used in this study will be defined. The methods for determining the LAI measurements are then described. These are the simple allometric equation, species-specific linear regressions, the ground scanning gap fraction method, and the field sampling method. The final section compares the roughness values obtained from the LAIs derived in this study, and these roughness values will be compared with values set out in guideline literature.

2. Methods

[7] In this study, three methods are used to extract leaf area indices of three riparian forest types defined in the following section. LAI values are necessary when calculating roughness of riparian forests with full foliage (section 2.2). Those indices derived from allometry and linear regressions can only provide estimates of the full tree LAI, without consideration of stage-dependent vegetation roughness. Terrestrial

laser scanning is necessary to first determine the LAI in the field, as well as assessing a stage-dependent area that comes in contact with floodwater.

2.1. Scanning Sites

[8] Using TLS, three forest sites were scanned along the Garonne River (SW France) on 6 June 2006, all within 300 m of the river channel. The Garonne floodplain consisted mostly of commercial hybrids poplars (of *Populus × euramericana*) with many clones (same genetic stock) in homogeneous plantations, as well as limited riparian natural woodlands of black poplar (*Populus nigra*) in more heterogeneous-sized patches. The three forest cover type included young (Y) and mature (M) planted poplars as well as mature natural poplar (N). The young planted poplar plot consisted of 56 trees with an area of around 0.45 ha. The mature and natural poplars consisting of 110 and 95 trees, with areas of 0.9 and 0.2 ha, respectively. The young and mature planted poplars were almost evenly spaced, while the natural poplars where very chaotic in space as would be expected in an immediate riparian zone of natural woodland.

[9] The TLS used in this study can be described as a remote sensing technique with the power to rapidly extract extremely dense spatial data. TLS has the capability to scan an object or objects in 3-D from various positions resulting in a very good spatial coverage with limited shadowing effects. This research used a Leica Geosystems High Definition Surveyor (HDS 3000 scanner head) to collect data and were analyzed using the Cyclone 5.5 software. This instrument has a good pulse recovery larger than 100 m with a distance range from 0.5 to 300 m and a field of view of 360° in the horizontal and 270° in the vertical. The effective scan distance was around 50 m for the planted poplar forest and 15–20 m for the natural riparian forest. Further details of the technique is given by *Antonarakis et al.* [2009] as well as *Frei et al.* [2005]. Multiple scans were performed at each site in order to have the best coverage of the forest canopies and their leafy crowns. Each site was therefore scanned at four to five different locations. Resolutions of 10 cm were chosen for the planted poplar sites and 5 cm for the natural riparian site.

2.2. Estimation of Vegetative Roughness

[10] The effect of leaves on vegetation roughness is not well understood, and they are accordingly often ignored. A significant contributor to drag of most trees in above canopy flows is the drag of leaves. This suggests that the leaf area and leaf density are important parameters in determining the overall resistance of a forested stand. *Järvelä* [2004] used the leaf area index but also added a second parameter to account for the flexibility of vegetation. This second parameter is defined as the dimensionless vegetation parameter "α" that accounts for the deformation effect of plants in a flow. According to *Fathi-Moghadam* [1996], α can be related to velocity, as the friction factor is a power function of flow velocity, so that $\alpha = (U/U_\chi)^\chi$, where the parameter χ is unique for a particular species and U_χ is the lowest velocity used in determining χ (typically 0.1 m/s). The resulting flow resistance equation for considering leafy woody vegetation is

$$f = 4C_{d\chi}\left(\frac{U}{U_\chi}\right)^\chi \times \text{LAI}(h). \tag{1}$$

[11] In equation (1), $C_{d\chi}$ and the one-sided LAI (leaf area index) are used to describe the vegetation properties and are used instead of the vegetation index (ξE) described by *Kouwen and Fathi-Moghadam* [2000]. The LAI may not be nonlinear due to the vertical heterogeneity of canopies, so the projected leaf area on floodwater is a function of the flood-water flow depth (h) until full submergence of the canopy. $C_{d\chi}$ is the drag coefficient for a leafy tree and is specific to individual tree species. The leaf area stated above does not increase linearly with an increase in height or flow depth, so cumulative leaf area relative to the flow depth is needed and will be different for different species and tree spacing. The vegetation parameter (χ) can be defined further as the frequency-length exponent originally identified by *McMahon and Kronauer* [1976]. This is the least squares fit of the power function relationship between the maximum length of elastic branches and their natural frequency (number of cycles per minute at the lowest mode of vibration). *McMahon and Kronauer* [1976] performed a large number of branch frequency experiments with different species and subspecies of trees including poplars, maples, larches, and oaks. An overall value of all trees measured for χ was calculated as –0.59, with the value obtained for all poplars being averaged as –0.60. Alternative drag formulations are common in terrestrial and aquatic canopy literature, where the drag force is related to the fluid velocity, drag coefficient, and the reference area ($F_d = 0.5\rho U^2 C_d A$).

[12] The species-specific drag coefficient ($C_{d\chi}$) is normally estimated from literature values based on flume experiments using leafy vegetation. The resulting drag coefficients obtained from different studies vary based on the method and the size of the vegetation as well as the species studied. The drag coefficient defined and used in the previous study by *Antonarakis et al.* [2009] is also used here and is expressed as

$$C_d = \frac{2K_o R_h^{-k} V}{A_{p,tot} s}.$$ (2)

[13] In equation (2) K_o is the multiple regression constant, R_h is the Reynolds number based on flow depth, s is the average spacing between vegetation elements, and the exponent (k) is another regression coefficient developed by *Tsihrintzis* [2001] which ranges from 0.6 for increasing vegetation frontal area with depth to 1.5 for decreasing frontal area with depth. According to *Lee et al.* [2004] with turbulent flow ($R > 10,000$), the product of the two variables $K_o R_h^{-k}$ can be assumed to be 0.15–0.2. Equation (2) also includes V as the total volume occupied by the canopy. The full vegetation projected area $A_{p,tot}$ (i.e., the reference projected area of the fully submerged tree) accounts for the leaf area (LA) as well as the consideration of the bark frontal area (A_b), which also accounts for the trunk.

$$A_{tp} = LA + A_b.$$ (3)

[14] Equation (1) can be solved iteratively to define the friction factor f with each desired flow depth (h). This is achieved once the values of $C_{d\chi}$, LAI, χ, and U_χ are known either from literature or from actual measurements. The first iteration involves inserting an initial estimate for the velocity (U) if it is unknown for a certain depth of flow in a specific

flood event. The resulting friction factor f in equation (1) is input to the Darcy-Weisbach equation to calculate a new velocity. The Darcy-Weisbach equation is shown below:

$$U = \sqrt{\frac{8ghS}{f}}.$$ (4)

[15] For wide cross sections, the hydraulic radius can be estimated to be the flow depth (h) [*Järvelä*, 2004]. The flow depth will be related to the cumulative LAI, so each increase in LAI with height will cause an increase in flow depth. The acceleration due to gravity (g) is 9.81 m/s^2, and the slope of the channel (S) can be measured for each specific reach. The velocity calculated with the Darcy-Weisbach equation can then be replaced in the desired resistance equation (equation (1)). The iteration is then repeated until the velocity does not change. The final resistance for a specified flow depth is then the friction factor calculated with the converged velocity.

2.3. Determining the LAI

2.3.1. LAI From Allometric Regression

[16] A principle source that has considered allometric regressions between large numbers of vegetation properties for a very large number of tree species is the work presented by *Niklas* [1994]. One of the relationships defined by *Niklas* [1994] considers the scaling relations between leaf area (LA in cm^2) and the diameter at breast height (D in cm). An allometric power law was determined for 46 North American deciduous species with unlobed and lobed simple leaves, palmate leaves, and pinnate leaves. The final regression of the data revealed the isometric power law as

$$LA = 917D^{1.98 \pm 0.05}.$$ (5)

[17] The diameters at breast height (dbh) used in this study were obtained from ground surveys in June 2006, at the same time as the TLS data acquisition. The leaf area was computed as a mean value resulting from all trunk diameters in each plot.

2.3.2. LAI From Species Specific Regressions

[18] Species-specific linear regressions were also used in this study for further comparison. A limited amount of literature deals with regressing aspects of the hybrid poplar leafy canopy with tree height, or trunk diameter, and especially of mature poplars. A comprehensive study offered by *Gielen et al.* [2001] investigated linear regressions between the trunk diameter (in the form of the basal area (BA) in cm^2) and the total leaf area (m^2) for 89 *Populus × euramericana* hybrids and 92 *Populus nigra* trees with an R^2 value of around 0.93 for both:

$$LA = 0.2019BA \quad (Populus \times euramericana) \quad \text{and}$$
$$LA = 0.3519BA \quad (Populus\,nigra).$$ (6)

[19] This study was preferred as it gave a regression for the same hybrid poplar as well as for black poplar. Also, contrary to other studies which consider infant poplar seedlings [*Barigah et al.*, 1994; *Ceulemans et al.*, 1993], the hybrid poplars in the study of *Gielen et al.* [2001], although young,
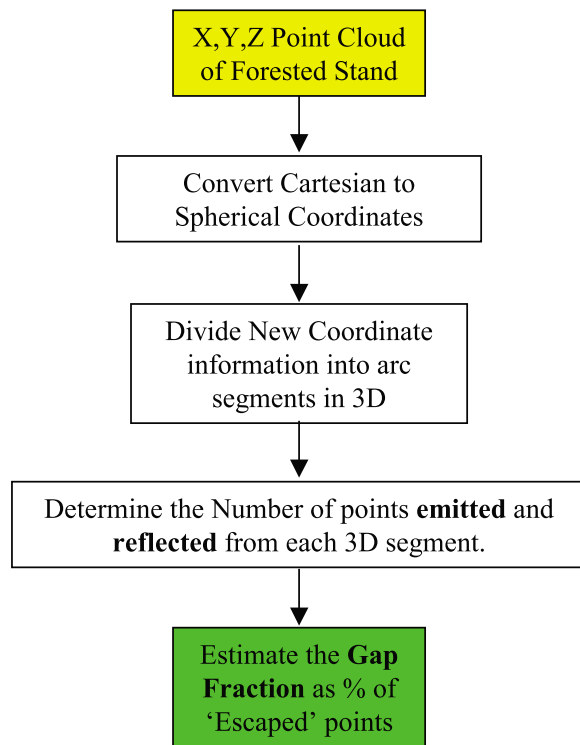
Figure 1. Flowchart describing the algorithm extracting gap fractions from scan data.

were considered up to 6 m in height. As for the previous section, the diameters at breast height used were obtained from the June 2006 surveys. The leaf area was again computed as a mean value resulting from all trunk diameters in each plot.

2.3.3. LAI From a Tree (Field Sampling)

[20] The leaf area index of a mature planted poplar tree in the M site was calculated by relating the specific leaf area (SLA) of the poplar clone *Dorskamp* with the dry mass of all the leaves present on this individual tree which was cut and weighted. The *Dorskamp* clone was felled from its lowest point in order to consider its full aboveground mass. It was felled in the month of June in 2007, so that the resulting LAI would be similar to terrestrial scanning data. Then each branch originating from the trunk was numbered and separated. The recognition of each of these branches was important first for identifying large branches that were cut more than two times and second for remembering which branches had been weighed. The trunk was also divided into multiple pieces to facilitate transportation. Subsequently, all the individual branches including the leaves, as well as the trunk pieces, were weighed and recorded. The mass of each component was measured using a 50 kg scale with an accuracy of measurement of around 50–100 g. For 10 of the branches originally attached to the main trunk, the wet leaf weight was also recorded separately in order to create a ratio of bark and leaf mass. The average leaf mass percentage for the 10 branches was then applied for all of the 21 main branch masses to estimate the total wet leaf mass of the tree. Finally, the dry leaf mass for the leaves removed from the six branches was established. With the percentage drying of the leaves as well as an estimate of the total wet leaf mass, the LAI was calculated using the specific leaf area and the mass of the dry leaves. The equation is as follows:

$$LAI = \frac{SLA \times LM_{dry}}{2 \times CA}. \tag{7}$$

[21] The specific leaf area (SLA in $m^2\ g^{-1}$) was obtained for the *Dorskamp* clone from research undertaken by *Monclus et al.* [2005]. The total leaf area of the plant can be obtained by multiplying the SLA with the dry leaf mass (LM_{dry} in g). Subsequently, the one-sided leaf area index is achieved by halving the leaf area and dividing it by the horizontal canopy area (CA in m).

[22] The field sampling LAI was done for one mature tree only, due to a lack in equipment, time, and permission on the site. Therefore, this may be considered a limitation to our methodology, similar to the lack in field information in the TLS-LAI method described by *Strahler et al.* [2008].

2.4. Extracting Total and Stage-Dependent LAI From TLS

[23] Traditional methods for measuring the LAI have focused in part on obtaining gap fractions from vegetated areas and applying them to transmittance relationships such as the Beer-Lambert law [*Nel and Wessman*, 1993]. Some of the methods to obtain gap fractions are somewhat invasive or damaging to the vegetation, time consuming, and labor intensive [e.g., *Peper and McPherson*, 2003; *Weiss et al.*, 2004]. The canopy gap fraction can be defined as the probability that a ray of light or a pulse of energy will pass through the canopy without encountering foliage or other plant elements [*Danson et al.*, 2007]. Therefore, a gap fraction of 0% would mean that incoming radiation was intercepted completely by the canopy. One of the most widely used methods for determining the gap fraction of a vegetated patch is hemispherical photography, which provides a permanent 2-D record of the canopy structure. Terrestrial laser scanning is ideal as a substitute for photographic methods as it can describe a vegetated area in an interactive 3-D data set, scanning from the ground and looking up. In this study, a specific method has been developed for using terrestrial scan data in order to determine the gap fractions of various stands with foliage and to subsequently estimate the total and stage-dependent LAI. The method is presented.

2.4.1. Extracting Gap Fraction From TLS

[24] *Danson et al.* [2007] were among the first to extract canopy gap fractions from TLS data, and the method developed in this study has its origins in the idea of transforming the point cloud data set from Cartesian coordinates to spherical coordinates in order to be similar to hemispherical photography. The algorithm that will be described in this study is presented as a simple flowchart in Figure 1.

[25] In order to represent a complex forested stand fully, relatively large areas (between 0.3 and 1.2 ha) were chosen to scan canopies with their summer foliage. It was desired to obtain gap fractions for different segments of a forest canopy at various transmittance arcs from the scanner head (e.g., Figure 2). The first step in achieving this was to convert the data from Cartesian to a Spherical coordinate system. Spherical coordinates are needed in order to create equal arc segments from the scanner head position, where an increase
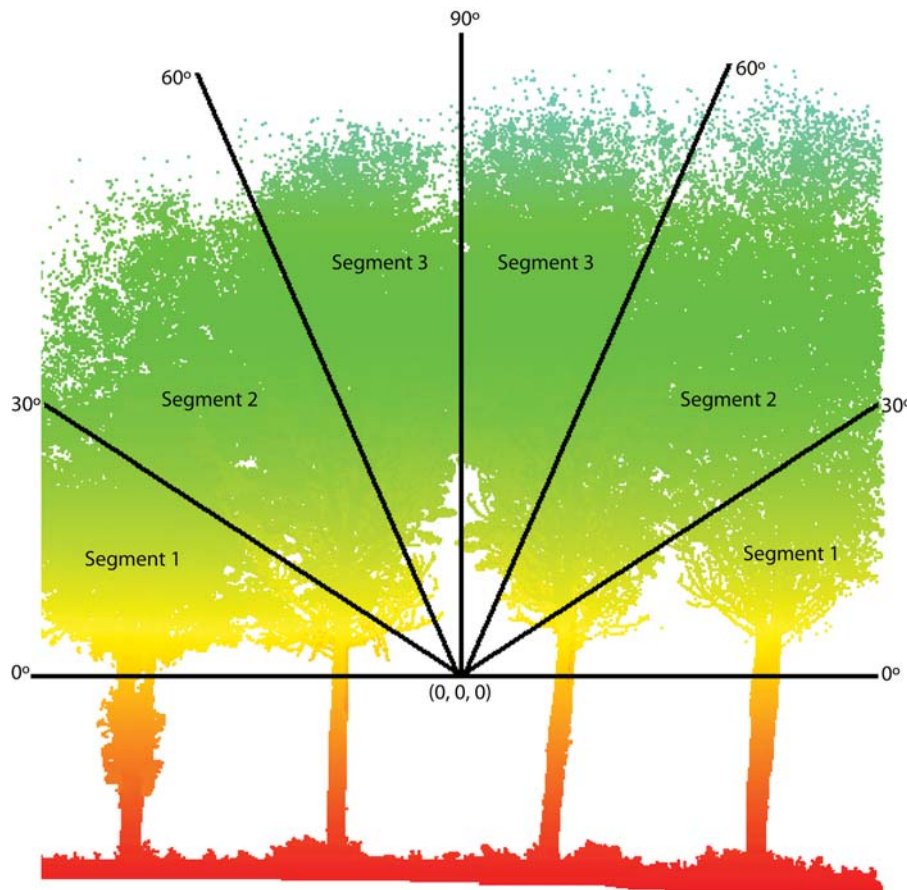
Figure 2. Segments extracted from a scanned section in the mature poplar forest. The segments are overlain on the original Cartesian point cloud. The shading schemes represent an increase in relative height.

in phi (φ) is equivalent to an increase in angle as in hemispherical photography, where the ordinate values are from 0° to 90°. The conversion from Cartesian to spherical coordinates is described as

$$\rho = \sqrt{(x^2 + y^2 + z^2)}, \qquad (8)$$

$$\varphi = a \cos \left(z/\rho \right), \qquad (9)$$

$$\theta = a \tan \left(y/x \right). \qquad (10)$$

[26] In equations (9) and (10), the phi (φ) axis represents the vertical angles from the origin. Therefore, a sphere of emitted points (mimicking the method of pulse emissions from the terrestrial lidar) can subsequently be divided into a number of user defined arcs. These arcs signified slices from the scanner head, being similar to half-circular segments of hemispherical photography. An illustrated example of three segmentations every 30° is presented in Figure 2 below in a 2-D frame (in this study segments were taken every 10°, with Figure 2 being illustrative only). From the base of the canopy level to the tips of the treetops, a number of arcs were then chosen and the number of points in each was counted.

[27] The final step before calculating the gap fractions per segment was to obtain the number of pulses emitted from the terrestrial laser scanner at a given probing distance with a specific resolution. This can easily be recorded from the Cyclone scanning program, which states the number of pulses emitted just before each scanning exercise. Thus, starting with the total number of points emitted from the scanner and the number of pulses returned to the scanner head in that arc, the gap fraction could be calculated, and the LAI could be calculated using the Beer-Lambert transmittance law.

2.4.2. Calculating the LAI From TLS Gap Fractions

[28] The method that will be used in relation to the gap fraction measurements based on ground scanning is the Beer-Lambert law originally proposed by *Monsi and Saeki* [1953]. The Beer-Lambert law incorporates the light transmission or gap fraction and the light extinction coefficient. To solve for the total LAI, the equation takes the form

$$\text{LAI} = \frac{-\ln(T_i)}{K}, \quad \text{where} \quad K = \frac{1}{2 \cos \theta}. \qquad (11)$$

[29] The variable θ is the angle at which the energy is transmitted (T_i) through the canopy. The law assumes that the foliage is randomly distributed or spherically distributed [*Anderson*, 1971], and in equation (11), the angles of foliage inclination are not needed. About the choice of the energy transmittance angle (θ), *Nel and Wessman* [1993] conclude that gap fraction measurements should be taken closest to solar noon, and typical measurements using various instruments are usually taken directly under a tree crown. For

Vertical Variation in Foliage
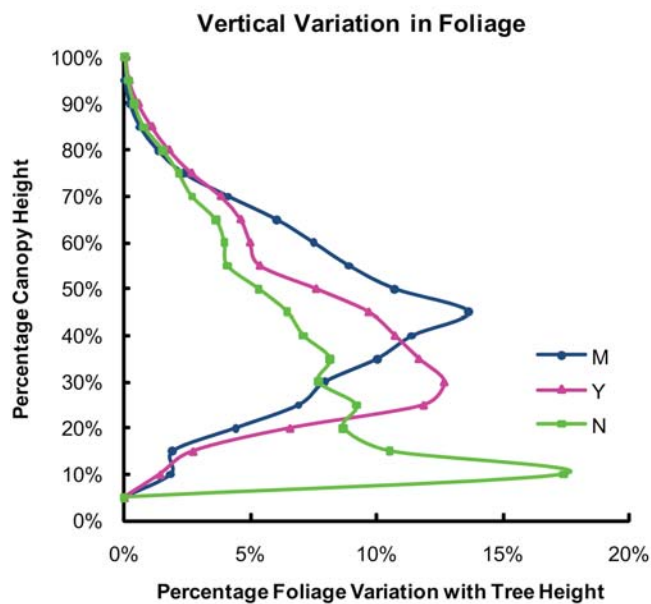
Figure 3. Variation of canopy foliage with tree height in the three poplar stands.

terrestrial scanning, this is not an option, as confirmed by *Danson et al.* [2007], as this would involve too much pulse return from the bark and branches. An advantage with TLS, though, is that it can gain canopy information for a whole forested stand rather than just from one tree. Therefore, it could return pulses from the densest part of the stand canopy, considering more foliage that just considering transmission through one tree. Equation (11) was applied to the three poplar forest types on the Garonne to calculate their total LAI for use in the resistance equations. However, floodwater does not always fully submerge a canopy, and accordingly, the cumulative, stage-dependent LAI needs to be established.

2.4.3. Calculating Stage-Dependent LAI

[30] For the purpose of determining the roughness of leafy vegetation, the stage-dependent leaf area index needed to be determined, as floodwater rarely submerges the full canopy layer. The allometry and linear regression methods presented in this study have the limitation that they can only give information on the total rather than a stage-dependent LAI. This is because the techniques do not have any detailed 3-D forest structure capabilities. Therefore, as given by *Järvelä* [2004], total leaf area indices could only be assumed to be distributed linearly with height.

[31] Foliage in canopies is in fact heterogeneously distributed with height, and the advantage of using TLS to define LAI with height is that it is an active 3-D remote sensing technique. Flow comes in contact with vegetation horizontal in space (in the x-y plane) or perpendicular to the ground. Therefore, TLS arc segmentation as described previously in this study and as illustrated in Figure 2 cannot easily be used as it is angularly not horizontally stratified. As expressed earlier in this study, scans were done for forest stands rather than for individual trees in order to limit the sampling error. For the purpose of determining the leaf proportion with canopy height (or flow depth), more than one scan was considered per site in order to get full coverage of the forested areas considered. Hence, for each site, four to five scans were done with the same resolution defined in section 2.1.

Extracting the percentage of foliage with increase in height follows a few steps, subsequent to obtaining and geo-registering all the scans to the WGS84 coordinate system. First, 10×10 m subgrids were cut from each forest site in order to have an even ground surface. This resulted in around 45, 90, and 20 subgrids from the young planted, mature planted, and natural poplar forests. From each of these sub-gridded sites, large central trunks were manually removed where possible to maximize the return from foliage. Then, each of the around 155 sites containing point clouds of foliage hits were input into an algorithm that determined the minimum and maximum canopy elevations, divided the point cloud into 20 vertical segments, determined the lidar returns per segment, and finally obtained each segment point cloud proportion (i.e., gap fraction). Subsequently, each of the 20 vertical point cloud proportions were averaged with all other subgrid sites of the same forest type. The final percentage foliage variation with percentage canopy height is presented in Figure 3. These percentages were then applied to the total LAIs determined from the TLS-LAI technique along with the known canopy heights to get representative stage-dependent LAIs for the three forest sites.

3. Results and Discussion

3.1. Comparison of the LAI Estimates

[32] For the field sampling method, the average mass proportion of wet leaves on the wet branches was measured to be around $27.65\% \pm 6.8\%$. The total mass of the wet branches was measured to be 524.00 kg, with the weight of the trunk being 922.11 kg. Therefore, the wet leaf mass was estimated to be on average 144.89 kg. After the complete drying of the sample of leaves cut off from the 10 branches, the proportion of water loss was calculated to be 64.3% of the original wet leaf weight. This is in line with the Food and Agriculture Organization document [*FAO*, 1979] that stated 60% of the leaf mass in poplars can be accounted for by the moisture content. Therefore, the dry leaf mass was finally estimated to an average of 51.73 kg. Taking all of these factors into account, the final LAI of the mature poplar clone was calculated to be LAI = 4.19 ± 1.03. This field sampling value for mature planted poplars can now be compared to the values obtained from the other methods.

[33] The resulting LAI values for all method described in this study are presented in Table 1. A limitation with the allometric equation presented by *Niklas* [1994], even if it can be considered an important base equation, is that a very large number and species of trees were used to create the regression, which may not accurately apply to any single species. The mature poplar LAI values up to 3.1 times smaller than the field sampling values, with an average of 1.9 times smaller. The standard deviations of the natural poplar forests

Table 1. LAI Values Derived for the Three Sites for All Methods Described in This Study[a]

Site	Allometry	Linear Regression	TLS Gaps	Field Sampling
Y	0.96 ± 0.18	1.42 ± 0.53	0.97 (0.95–0.99)	
M	2.24 ± 0.57	3.72 ± 0.91	4 (3.25–5.42)	4.19 ± 1.03
N	3.91 ± 2.56	5.56 ± 3.4	4.25 (3.69–5.02)	

[a]These calculations are for the young (Y) and mature (M) planted poplars and for the natural poplars (N).

Gap Fraction Distributions
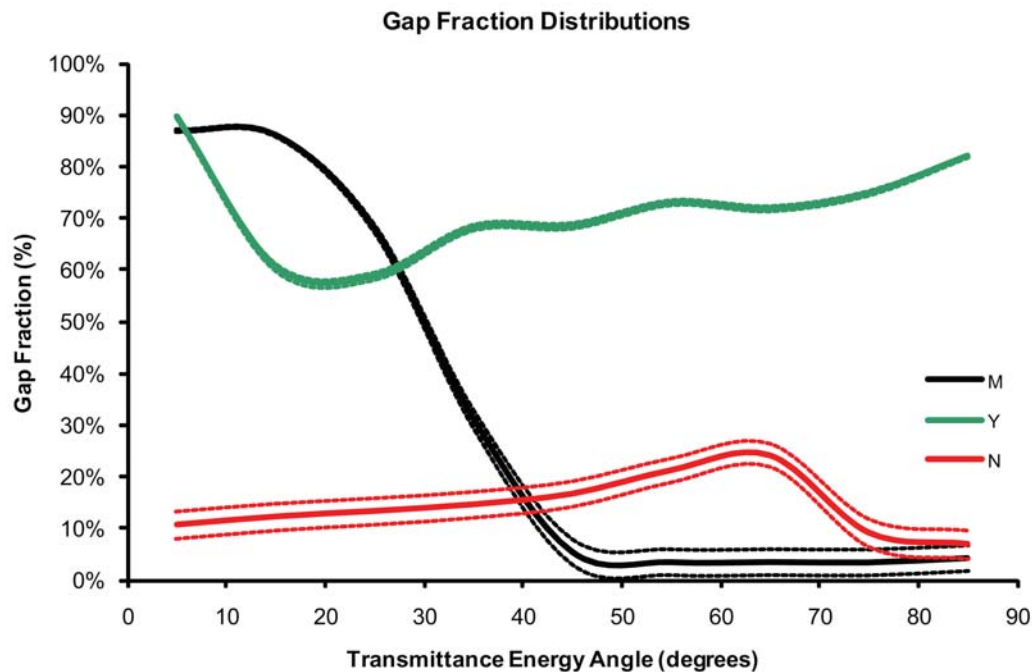
Figure 4. Gap fraction distributions for the three forested sites scanned with the presence of leaves. The mature (M) and young planted forest (Y) and the natural forest (N) all have dotted lines. These represent the 5 and 10 cm point resolution for the natural and planted forests, respectively.

are larger than for the planted poplar due to the stand density and heterogeneity of the individual tree sizes. The method by *Gielen et al.* [2001] produces closer LAI values when compared to the mature planted poplar sampling method, with average values around 11% smaller than the field sampling LAI and a maximum difference of 86%. Again, the standard deviations of the natural poplar forests are large due to the forest heterogeneity. These species-specific regressions may also be limited due to that they were formulated for younger poplars and also not for naturally growing plants.

3.2. LAI From Gap Fraction Method

3.2.1. Gap Fractions From TLS

[34] Gap fractions are presented for the three Garonne River sites where summer scans were taken in June 2006. The gap fraction variations for the three regions with the energy beam angle (θ_i) are presented in Figure 4. Gap fraction distributions in relation to transmittance angles have usually been characterized as having high fractions for lower angles and lower fractions for higher angles [*Norman and Campbell*, 1989]. The highest gap fractions shown by *Norman and Campbell* [1989] were between 30% and 50% for transmittance angles of 0°–30°, and the general trend of the distribution decreases from around 45°–60° until the lowest gap fractions of 0%–5% from 70°–90°. The only distribution from Figure 4 that is similar to this description is the dense mature planted poplar (M). Even here, however, the gap fractions at the lower angles are larger than *Norman and Campbell* [1989] imply. The other two distributions are characterized as having more consistent gap fractions across a wide range of transmittance angles, with young planted poplar (Y) having rather high (55%–75%) values and the natural poplar site (N) very low values (5%–20%).

[35] In fact, for dense forests such as pines, *Danson et al.* [2007] reported a similar issue when comparing the gap fractions derived from terrestrial scanning and hemispherical photography. They reported that for zenith angles above 50°, the differences between the distributions derived from the two methods were only around 5% of the gap fraction. For zenith angles below 50°, the disparities were larger with values up to 11%. Perhaps, very large gap fractions consider areas where the scanner pulse misses the tree crown.

[36] There was the need, therefore, to calculate the angles where the scanner recorded hits from the tree crown rather than from the trunks or from pollen and other particulate matter (which was very dense during the June 2006 field campaign). It was calculated that for the mature planted poplar (M), the scanner received pulse returns from the canopy from around 30°. For the young planted poplar (Y), the scanner received pulse returns from the canopy from around 10° until 45°. For the natural forest site (N), the scanner received pulse returns from the foliage for the full 90°. This last site has low gap fractions because of the density of leaves present from the low elevations of the trees. In fact, some of the trees scanned were bent from flooding, resulting in much of the foliage being nearer to the ground. These gap fraction results can now be used in the Beer-Lambert law.

3.2.2. Beer-Lambert Calculation

[37] The Beer-Lambert method can be applied to segmentation windows with a high density of points returned related to their transmittance angle (θ). For the mature planted poplar (M), the segments with the highest density of foliage were between 40° and 60°, or roughly in the central areas of the canopy. The young planted poplar (Y) presented the highest density of its foliage in the bottom half of the canopy from 10° to 30° from the scanner. In the natural forest section (N), the highest densities of points returned were at the lowest

Table 2. Drag Coefficients Defined for the Three Forested Areas Considering the Four Methods of Obtaining Leaf Area Indices, and for the Young and Mature Planted Poplars, and for the Natural Poplars

Site	Allometry	Linear Regression	TLS Gaps	Field Sampling
Y	0.403 ± 0.05	0.297 ± 0.07	0.401 ± 0.01	
M	0.666 ± 0.11	0.462 ± 0.09	0.437 ± 0.08	0.421 ± 0.085
N	0.142 ± 0.05	0.115 ± 0.05	0.135 ± 0.01	

angles from 0° to 20°. Using equation (11), the resulting LAI for the highest density of foliage in relation to their beam angles were calculated as LAI = 3.25–5.42 for the mature planted poplars, LAI = 0.945–0.990 for the young planted poplars, and LAI = 3.69–5.02 for the natural poplars. The average values were 4.00, 0.967, and 4.25 for the mature planted poplar, young planted poplar, and natural poplar, respectively.

[38] At first glance, the range and average LAI results for the mature planted poplars (VM) are very similar to the field sampling value. In fact, the values obtained here are within 5% of the field sampling values. In relation to the other two methods presented in this study, the results are closest to those obtained from the species-specific linear regression method with an average difference in values of around 8%.

[39] High-quality results have been recorded when using the Beer-Lambert law. *Nel and Wessman* [1993], using a line quantum sensor to measure transmittance, stated percentage differences between the field sampling values and the Beer-Lambert equation-derived LAIs of 5%–28% with an average of 14%. *Vose et al.* [1995] used the Beer-Lambert law on different mature hardwood stands and recorded a difference between the estimated and calculated values of between 7% and 15%. *Maass et al.* [1995] used the Beer-Lambert law on a number of tropical trees and measured the transmittance using a ceptometer (photosynthetic radiation sensor). The resulting LAI values correlated with the field sampling leaf litter calculation with an R^2 of 98%. *Solberg et al.* [2006] demonstrated that gap fractions could be obtained from airborne lidar using the instrument swath angle as the transmittance angle. The lidar was flown with a small swath width at an average height of 650 m, resulting in a spatial resolution of up to 10 points/m^2. The Beer-Lambert law was correlated to field measurements of LAI for 20 stands of Scots pine, with high R^2 values of 87%–93%. All of these methods demonstrate the success of the Beer-Lambert law, and its simplicity has been hailed in research such as that of *Duursma et al.* [2003]. Therefore, the resulting LAI values may be described as not depending on the method of obtaining the data but the calculations involved using those data.

[40] In this study, determining total LAI using the Beer-Lambert law based on ground scanning has produced equally good or better results compared the other studies described above (average of 5% from field sampling LAI value). Terrestrial laser scanning has now shown that it is able to extract meaningful information (gap fractions) and is also relatively quick in its data collection and manipulation (a couple of days from end to end). The advantage of TLS to other instruments is also that it is multifaceted and can be used to obtain information that is not solely for LAI measurements (such as spacing, trunk diameters, canopy heights, etc.). The derived LAI values can now be used to determine the roughness of forests in the summer.

3.3. Roughness for Leafy Vegetation

[41] The LAI and stage-dependent consideration of canopy density with foliage can now be applied to the resistance equation (equation (1)).

3.3.1. Drag Coefficient

[42] Using equation (2), the total projected area ($A_{p,tot}$) can now be defined as the bark area plus the total one-sided leaf area. The remaining criteria such as the element spacing were determined from the field data. Using the methods described in this study, the drag coefficients with the presence of leaves are shown in Table 2.

[43] The reason for calculating the drag coefficient for each individual forested area is that the values presented in the literature are limited to averages in a certain species. The values presented above are around $C_d = 0.3$–0.6, with the values for the natural forest being lower. *Järvelä* [2004] used a drag coefficient for leafy willows of 0.43; *Fathi-Moghadam* [1996] developed drag coefficients for various hardwoods from 0.56 to 0.59 and pines from 0.45 to 0.69; and *Rudnicki et al.* [2004] calculated drag coefficients for pines of around 0.4.

3.3.2. Manning's *n* Calculations for Leafy Forests

[44] Resistance values for leafy vegetation were calculated using equation (2), and the Darcy-Weisbach friction factors were converted into Manning's *n* values. The cumulative LAI values used for the TLS-LAI method result from the stage-dependent foliage proportion calculations. For the allometry and the linear regression methods, a linear cumulative LAI is used with height. The total roughness (leafy plus bark components) with increase in flow depth is presented in Figure 5d, as well as the leafy roughness components from the three forest stands. The first plots (Figures 5a–5c) have roughness values presented for the LAI values calculated for each method. The total roughness is the sum of the rigid leafless roughness, calculated from resulting roughness values presented by *Antonarakis et al.* [2009] and the roughness of the leafy component presented in this study. It should be noted that any flood as high as 15–20 m would involve extreme flood events and that resistance equations may not apply. In recent recorded history, though, only flooding of around 6 m was recorded for the river sites [*Muller et al.*, 2002]. The range of Manning's *n* values for the three forest sites can be determined at selected flow depths from when the floodwater comes into contact with the forest canopy. An example of values for flow depths of 4, 6, and 8 m is shown in Table 3.

[45] It is clear that using the TLS method for determining LAI results in the closest estimates of total LAI when compared to the field sample survey. It is also clear that the leafy roughness shown in Figures 5a–5c represents the heterogeneity in the vertical foliage distribution, which cannot adequately be represented simply assuming linear LAI distribution with height. The roughness values obtained in this study can be compared to guideline literature values such as that of *Chow* [1959] and the *USGS* [1989], with relevant values presented in Table 4. The depth of flow considered for the values presented in the table is not known, but nevertheless, they are relatively in concurrence with the values presented in this study. The range of roughness values for vegetation on floodplains is from around $n = 0.100$–0.200, with dense vegetation lining the channel edges rising higher to around $n = 0.030$–0.500. All of the three forest types are in close proximity to
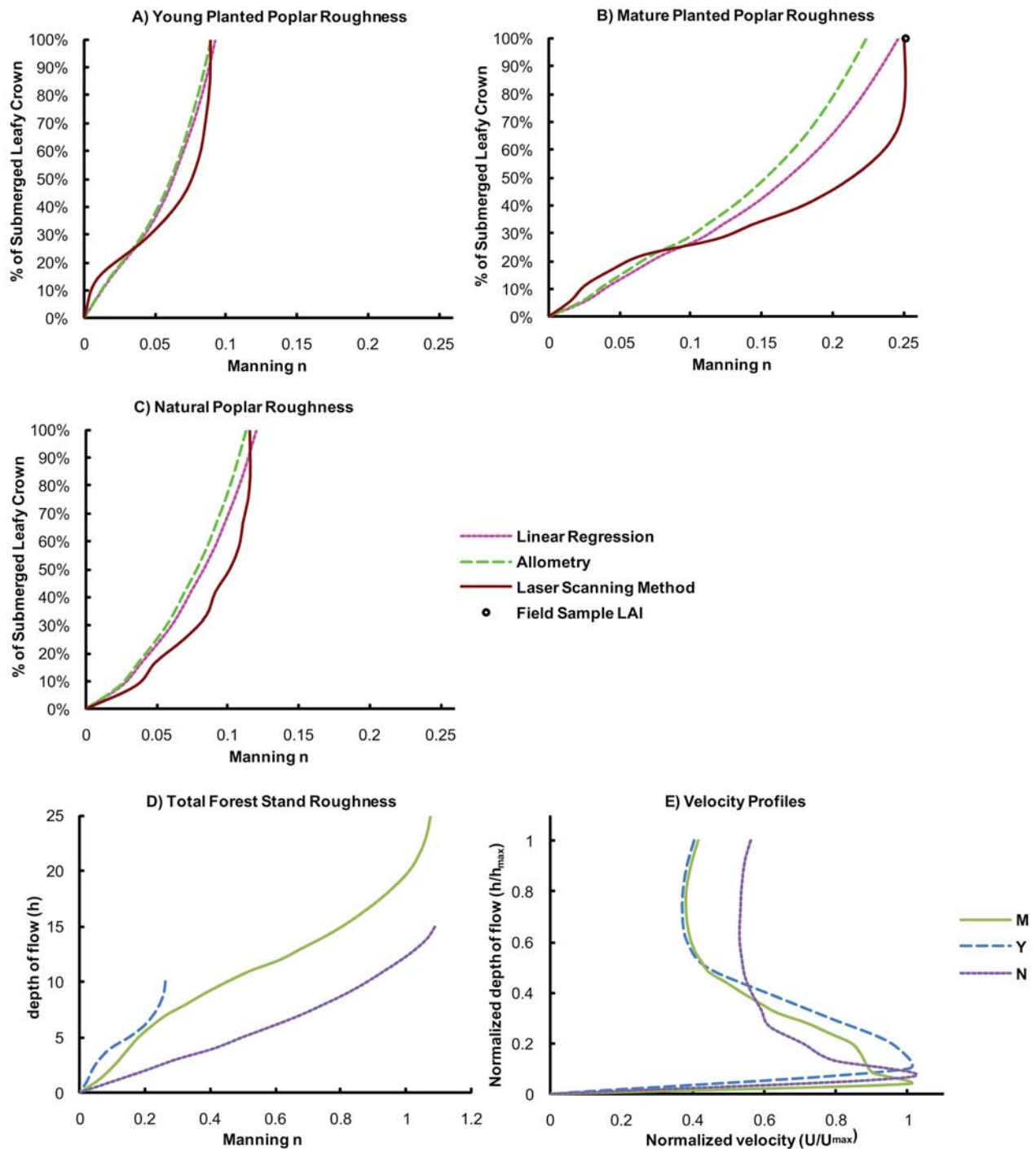
Figure 5. Manning leafy roughness coefficients considering the canopy of forest stands at all stages of their submergence. (a) The young planted poplars (Y) had a 7 m average crown height; (b) the mature poplars (M) had an 18 m average crown height; and (c) the natural poplars (N) had a 12 m average crown height. (d) The total roughness (woody + leafy) of the three stands considers the TLS gap fraction method. (e) The plot demonstrates the normalized velocity profiles derived from the three forest types.

the river channel, but the natural forest is the only forest type lining the channel. Roughness values from 4 to 6 m are within the range presented by *Chow* [1959] and only go above when the flow depth rises greater than 6 m. The planted poplars have lower roughness values for all flow depths con-

sidered, when compared to natural poplars; this is true both in terms of their total summer roughness and their foliage component. This is because a larger proportion of the leaf density is concentrated near the bottom of the canopy for natural forests.

Table 3. Manning's *n* Roughness Values for Three Different Flow Depths Considering the Full Tree Roughness (Leafy Plus Bark Components) and Its Leafy Component Separately[a]

Sites	4 m (Total)	4 m (Leaf)	6 m (Total)	6 m (Leaf)	8 m (Total)	8 m (Leaf)
Y	0.0946–0.0947	0.0095–0.0096	0.195–0.196	0.0684–0.0685	0.244–0.245	0.0856–0.0861
M	0.151		0.22		0.327–0.328	0.0151–0.0156
N	0.410–0.411	0.034–0.037	0.585–0.591	0.0670–0.0716	0.745–0.751	0.0882–0.0945

[a]Beer-Lambert LAI calculations are used for the young (Y) and mature (M) planted poplars and for the natural poplars (N).

[46] A few other studies have focused on acquiring total (leafy and woody) roughness values for vegetation, but little has been done for the leafy component. *Järvelä* [2002] performed flume experiments over willows that were 70 cm tall and obtained full plant roughness values of around $n = 0.120$–0.277. *McKenney et al.* [1995] estimated the roughness of dense natural mature willows in Missouri ranging from $n = 0.091$–0.140, for low levels of flow depth. For a flow of a couple of meters, *Rodrigues et al.* [2006] calculated the roughness of dense natural young poplars and willows in the Loire River from $n = 0.083$–0.102. *Anderson et al.* [2006] calculated the average roughness of tall vegetation such as forests to be around $n = 0.130$–0.150 for the first 4–5 m of flow on the floodplain.

[47] Studies have also attempted to simulate or retrieve the velocity profiles of floodwater around a representative tree or forest patch. This kind of information can be useful in validating the structure and resistance in this study, as there was no available flooding data for the Garonne River. Normalized velocity profiles were calculated for an increase in the normalized flow depth until full vegetation submergence. The profiles for the three forest stands are shown in Figure 5e. It is expected that for the planted forests, the velocity profiles will have an evident separation between the velocity around the trunk and in the leafy crown. This is especially evident for the mature planted poplars shown in Figure 5e, where the velocity begins to rapidly decrease once the flow enters the crown (30% of the depth). Further up in the canopy, the combination of a smaller frontal area increment and an increase in the stream power will result in velocity increases, at around 70%–80% for planted poplars and 60% for natural poplars (from Figure 5e). Most studies that attempt to derive velocity profiles resort to modeling or flume techniques. Yet even with representative vegetation structures, the velocity profiles in Figure 5e are very similar to those presented in studies by *Naot et al.* [1996], *Wilson et al.* [2003], *Yagci and Kabdalsi* [2008], and *Yang et al.* [2007]. *Yang et al.* [2007] performed flume experiments over eight structural tree types until full submergence and beyond. The velocity profile for all eight tree types increased and remained stationary until 20%–30% of the plants' height, where above this point the velocity decreased by 25%–35% maximum before starting to rise again near the tip of the canopy (75%–85% of the tree's height). *Yagci and Kabdalsi* [2008] demonstrated in-canopy velocity profiles of two vegetation types, *Pinus pinea* and

Thuja orientalis, using flume studies and calculations. Their resulting profiles revealed an increase and then constant velocity for the first 20% and 40% of the submerged flow depth for the two aforementioned species. This was followed by a rapid decrease in flow velocity within the crown. Velocity profiles of representative foliage canopies shown by *Wilson et al.* [2003] and *Naot et al.* [1996] show similar patterns.

4. Conclusions

[48] Field measurements and terrestrial laser scanning have been used in this study in order to determine the leaf area index of various forest types investigated near the Garonne and Allier rivers. Field measurements made on individual trees for all of the three forest sites were used in calculating the LAI from a general allometric and species-specific regression equations based on the trunk diameter. Terrestrial laser scanning was used innovatively as a mechanism to extract gap fractions from high-resolution summer point cloud data in order to eventually extract leaf area indices. The LAI of a single mature poplar tree on the Garonne was estimated by felling the tree and measuring the representative wet and dry mass of both the branch and leaf components. The stage-dependent LAI was related to the cumulative density of airborne and terrestrial lidar points over a forest stand of a certain type. Resulting leafy roughness (leafy and branch components) for the three sites fell within the range of values presented by the literature, although information on extreme flooding where the flow depth rises to the high levels of the canopy was not available. Roughness values for planted poplars ranged from around $n = 0.170$–0.195 and around $n = 0.245$–330 for in-canopy flow of 6 and 8 m, respectively. Roughness values for natural poplars were around $n = 0.590$ and around $n = 0.750$ for in-canopy flow of 6 and 8 m, respectively. Roughness values resulting only from the leafy component are difficult to compare with similar flow depths as canopies begin at different heights. Yet if the full canopies were submerged, then planted poplars would offer an average foliage roughness of around $n = 0.09$–0.25 for planted poplars of all ages and $n = 0.11$–0.12 for natural poplars of all ages, which accounts for around 20%–30% and 10% of the roughness for planted and natural poplar, respectively. Studies like that of *Järvelä* [2004] calculated larger roughness values of the leafy component, yet it should be considered

Table 4. Manning's *n* Values for Flow in Leafy Woody Vegetation on Floodplains or on the Channel Lining

Areas Described	Manning's *n* Range	Source
Heavy forested stand in floodplain with flow in the branches	0.100–0.160	*Chow* [1959]
Dense straight willows on floodplain with full foliage	0.110–0.200	*Chow* [1959]
Vegetal lining on channels	0.030–0.500	*Chow* [1959]
Heavy stand of leafy timber on floodplains with flood depth in branches	0.100–0.200	*USGS* [1989]

that the isolated willow measured was less than 0.7 m so that the proportion of leaves to bark would be much higher than for a taller tree. This also depends on the tree species.

[49] In this study, there were a couple of issues that require mentioning, with the first being the quality of the scanner data. A source of error with the ground scanning data is the effect of the wind. This would have the effect of too many points being reflected back to the scanner. Nonetheless, the scanning was performed on all occasions in the summer with limited weather anomalies. Another issue with the quality of scan data is that there would ultimately be pulses returned from the branches rather than only from the leaves. This is minimized by the fact that the scans were not taken underneath the canopies, which increases the chance of hitting a leaf, and scan returns were not considered in the lower parts of the canopy where the branches are thicker and more numerous. The field sampling method in this study was used to justify the remote sensing-derived LAI values, but this method in itself was estimated from proportions of the various tree components. Also, as described earlier, a limitation to our method was that we only had one field sampling tree for comparison. A final issue is that regardless of the data problems with scanning, it is successful in determining the gap fractions of forests, and therefore, the limiting factor in this study may well be the calculations and methods used in the final derivations of the LAI.

[50] The method for determining gap fractions in this study does not therefore guarantee that there will be no returns from the woody elements of the trees. In future research, this would need to be considered and corrected. For example, if scans of the same tree were done with the same resolution during the winter and summer months, then the total summer area could be subtracted from the total winter area of the tree, to obtain an estimate of the leaf area (leaf area = total canopy area − woody area). The terrestrial laser scanning technique to derive LAI in this study could also be applicable to shorter nonwoody vegetation but with an added difficulty. The TLS instrument stands on a tripod that can be around 1–1.5 m above the ground. Measuring the proportion of returns for vegetation underlying the instrument would require successfully separating the ground returns with foliage returns. This may prove difficult, especially in bushy vegetation, where the canopy starts from the ground.

[51] This study has developed the idea of the semi-automated extraction of the leaf area index of a selected forested site from an enormous amount of point cloud data with the help of various programming and data manipulation packages. Future research may be able to extract the total one-sided or two-sided leaf area from detailed scans of individual trees, so as to relate to the horizontal canopy area and create a LAI without having to choose between various techniques and methods. The strength of lidar remote sensing techniques means that the limit to parameterizing roughness in channels and floodplains may be the limit of the resistance equations and how they deal with extreme flow in leafy canopies. Nonetheless, this study has endeavored to provide information on the roughness of the complex riparian forests. This increase in knowledge for various riparian forests is necessary when considering roughness inputs of varying scales in hydraulic modeling. Information on final leaf-on vegetation roughness has been used in a further modeling study by *Antonarakis* [2008]. The overall scope of this modeling exercise was to illustrate the flooding effects of natural suc-

cession riparian reforestation. This was achieved by comparing river systems with drastically different channel and forest management techniques. In the first and second dimension of hydrologic modeling, meaningful information was extracted such as stage and discharge, as well as flow channelization and floodwater extent. Topographic boundary conditions were determined from lidar last pulse algorithms, with initial flood discharge obtained from governmental databases. Three-dimensional modeling was not performed, but the authors have used remote sensing techniques to extract complex vegetation structure, which is usually necessary as a physical boundary condition.

References

Anderson, B. G., I. D. Rutherford, and A. W. Western (2006), An analysis of the influence of riparian vegetation on the propagation of flood waves, *Environ. Modell. Software*, *21*(9), 1290–1296.

Anderson, M. C. (1971), Radiation and crop structure, in *Plant Photosynthetic Production: Manual of Methods*, edited by Z. Sestak, J. Catsky, and P. G. Jarvis, Dr. W. Junk, The Hague, Netherlands.

Antonarakis, A. S. (2008), The potential of lidar in recovering physical data on floodplain vegetation to parameterise flow resistance, Ph.D., Cambridge University, UK.

Antonarakis, A. S., K. S. Richards, J. Brasington, E. Muller, and M. Bithell (2008), Retrieval of vegetation fluid resistance terms for rigid stems using airborne lidar, *J. Geophys. Res.*, *113*, G02S07, doi:10.1029/2007JG000543.

Antonarakis, A. S., K. S. Richards, J. Brasington, and M. Bithell (2009), Leafless roughness of complex tree morphology using terrestrial lidar, *Water Resour. Res.*, *45*, W10401, doi:10.1029/2008WR007666.

Barigah, T. S., B. Saugier, M. Mousseau, J. Guittet, and J. Cuelemans (1994), Photosynthesis, leaf area and productivity of 5 poplar clones during their establishment year, *Ann. Sci. For.*, *51*(6), 613–625.

Ceulemans, R., J.-Y. Pontailler, and J. Guittet (1993), Leaf allometry in young poplar stands: Reliability of leaf area index estimation, site and clone effects, *Biomass Bioenergy*, *4*(5), 315–321.

Chow, V. Y. (1959), *Open Channel Hydraulics*, McGraw-Hill, New York.

Clawges, R., L. Vierling, M. Calhoon, and M. Toomey (2007), Use of a ground-based scanning lidar for estimation of biophysical properties of western larch (*Larix occidentalis*), *Int. J. Remote Sens.*, *28*, 4331–4344.

Curran, P. J. and H. D. Williamson (1987), Estimating the green leaf area index of grassland with airborne multispectral scanner data, *Oikos*, *49*, 141–148.

Cutini, A., G. Matteucci, and G. S. Mugnozza (1998), Estimation of leaf area index with the Li-Cor LAI 2000 in deciduous forests, *For. Ecol. Manage.*, *105*(1–3), 55–65.

Danson, F. M., D. Hetherington, F. Morsdorf, B. Koetz, and B. Allgower (2007), Forest canopy gap fraction from terrestrial laser scanning, *IEEE Geosci. Remote Sens. Lett.*, *4*(1), 157–160.

Deblonde, G., M. Penner, and A. Royer (1994), Measuring leaf area index with the Li-Cor LAI-2000 in pine stands, *Ecology*, *75*(5), 1507–1511.

Duursma, R. A., J. D. Marshall, and A. P. Robinson (2003), Leaf area index inferred from solar beam transmission in mixed conifer forests on complex terrain, *Agric. For. Meteorol.*, *118*(3–4), 221–236.

FAO (1979), Poplars and Willows, FAO Forestry Series No. 10, pp. 328.

Farid, A., D. C. Goodrichb, R. Bryantb, and S. Sorooshianc (2009), Using airborne lidar to predict leaf area index in cottonwood trees and refine riparian water-use estimates, *J. Arid Environ.*, *72*, 1–15.

Fathi-Moghadam, M. (1996), Momentum absorption in non-rigid, non-submerged, tall vegetation along rivers (Doctoral thesis), University of Waterloo, Canada.

Fathi-Moghadam, M. and N. Kouwen (1997), Nonrigid, nonsubmerged, vegetative roughness on floodplains, *J. Hydraul. Eng.*, *123*(1), 51–57.

Frei, E., J. Kung, and R. Bukowski (2005), High definition surveying (HDS): A new era in reality capture, *Int. Arch. Photogramm., Remote Sens.*, *XXXVI*(8/W19), 204–208, CD-ROM.

Gielen, B., C. Calfapietra, M. Sabatti, and R. Ceulemans (2001), Leaf area dynamics in a closed poplar plantation under free-air carbon dioxide enrichment, *Tree Physiol.*, *17*, 1245–1255.

Järvelä, J. (2002), Flow resistance of flexible and stiff vegetation:A flume study with natural plants, *J. Hydrol.*, *269*(1–2), 44–54.

Järvelä, J. (2004), Determination of flow resistance caused by nonsubmerged woody vegetation, *Int. J. River Basin Manage.*, *2*(1), 61–70.

Jonckheere, I., S. Fleck, K. Nackaerts, B. Muys, P. Coppin, M. Weiss, and F. Baret (2004), Review of methods for in situ leaf area index determination: Part I. Theories, sensors and hemispherical photography, *Agric. For. Meteorol.*, *121*(1–2), 19–35.

Lovell, J. L., D. L. B. Jupp, D. S. Culvenor, and N. C. Coops (2003), Using airborne and ground-based ranging lidar to measure canopy structure in Australian forests, *Can. J. Remote Sens.*, *29*(5),607–622.

Kouwen, N. and M. Fathi-Moghadam (2000), Friction factors for coniferous trees along rivers, *J. Hydraul. Eng.—ASCE*, *95*(IR2), 329–342.

Kouwen, N. and R. M. Li (1980), Biomechanics of vegetative channel linings, *J. Hydraul. Div.— ASCE*, *106*(HY6), 1085–1103.

Lee, J. K., L. C. Roig, H. L. Jenter, and H. M. Visser (2004), Drag coefficients for modeling flow through emergent vegetation in the Florida Everglades, *Ecol. Eng.*, *22*, 237–248.

Maass, J. M., J. M. Vose, W. T. Swank, and A. Martinez-Yrizar (1995), Seasonal changes of leaf area index (LAI) in a tropical deciduous forest in west Mexico, *For. Ecol. Manage.*, *74* (1–3), 171–180.

McKenney, R., R. B. Jacobson, and R. C. Wertheimer (1995), Woody vegetation and channel morphogenesis in low-gradient, gravel-bed streams in the Ozark Plateaus, Missouri and Arkansas, *Geomorphology*, *13*, 175–198.

McMahon, T. A. and R. E. Kronauer (1976), Tree structures: Deducing the principle of mechanical design, *J. Theor. Biol.*, *59*, 443–466.

Monclus, R., E. Dreyer, F. M. Delmotte, M. Villar, D. Delay, E. Boudouresque, J. M. Petit, M. Marron, C. Brechet, and F. Brignolas (2005), Productivity, leaf traits and carbon isotope discrimination in 29 *Populus deltoides* × *P. nigra clones. New Phytol.*, *167*(1), 53–62.

Monsi, M. and T. Saeki (1953), Uber den Lictfaktor in den Pflanzengesellschaften und sein Bedeutung fur die Stoffproduktion, *Jpn. J. Bot.*, *14*, 22–52.

Muller, E., H. Guilloy-Froget, N. Barsoum, and L. Brocheton (2002), *Populus nigra* L. en vallée de Garonne: Legs du passé et constraints du présents, *C. R. Biol.*, *325*, 1129–1141.

Naot, D., I. Nezu, H. Nakagawa (1996), Hydrodynamic behavior of partly vegetated open channels, *J. Hydraul. Eng.—ASCE*, *122*(11), 625–633.

Nel, E. M. and C. A. Wessman (1993), Canopy transmittance models for estimating forest leaf area index, *Can. J. For. Res.*, *23*, 2579–2586.

Niklas, K. J. (1994), *Plant Allometry: The Scaling of Form and Process*, 395 pp., Univ. of Chicago Press, Chicago, Ill.

Norman, D. J. and G. S. Campbell (1989), Canopy structure, in *Plant Physiological Ecology: Field Methods and Instrumentation* edited by R. W. Pearcy, Chapman and Hall, New York.

Peper, P. J. and E. G. McPherson (2003), Evaluation of four methods for estimating leaf area of isolated trees, *Urban Foresting and Urban Greening*, *2*, 19–29.

Roberts, D. S., T. J. Dean, D. L. Evans, J. W. McCombs, R. L. Harrington, and P. A. Glass (2005), Estimating individual tree leaf area in loblolly pine plantations using lidar-derived measurements of height and crown dimensions, *For. Ecol. Manage.*, *213*(1–3), 54–70.

Rodrigues, S., J. G. Breheret, J. J. Macaire, F. Moatar, D. Nistoran, and F. Juge (2006), Flow and sediment dynamics in the vegetated secondary channels of an anabranching river: The Loire River (France), *Sediment. Geol.*, *186*, 89–109.

Rudnicki, M., S. J. Mitchell, and M. D. Novak (2004), Wind tunnel measurements of crown streamline and drag relationships for three conifer species, *Can. J. For. Res.*, *34*, 666–676.

Solberg, S., E. Naesset, K. H. Hanssen, and E. Christiansen (2006), Mapping defoliation during a severe insect attack on Scots pine using airborne laser scanning. *Remote Sens. Environ.*, *102*, 364–376.

Strahler, A. H., et al. (2008), Retrieval of forest structural parameters using a ground-based lidar instrument (Echidna (R)). *Can. J. Remote Sens.*, *34*, 426–440.

Tsihrintzis, V. A. (2001), Discussion of Wu et al., 1999, *J. Hydraul. Eng.*, *127*(3), 241–244.

USGS (1989), Guide for selecting Manning's roughness coefficients for natural channels and flood plains, *Water Supp. Pap. 2339*, USGS, Denver, Colo.

Vose, J. M., B. D. Clinton, N. H. Sullivan, and P. V. Bolstad (1995), Vertical leaf area distribution, light transmittance, and application of the Beer-Lambert law in four mature hardwood stands in the southern Appalachians, *Can. J. Remote Sens.*, *25*(6), 1036–1043.

Weiss, M., F. Baret, G. J. Smith, I. Jonckheere, and P. Coppin (2004), Review of methods for in situ leaf area index (LAI) determination— Part II: Estimation of LAI, errors and sampling, *Agric. For. Meteorol.*, *121*(1/2), 37–53.

Wilson, C. A. M. E., T. Stoesser, P. D. Bates, and A. Batemann Pinzen (2003), Open channel flow through different forms of submerged flexible vegetation. *J. Hydraul. Eng.—ASCE*, *129*(11), 847–853.

Yagci, O. and M. S. Kabdalsi (2008), The impact of single natural vegetation elements on flow characteristics, *Hydrol. Processes*, *22*, 4310–4321.

Yang, K., C. Shuyou, and D. W. Knight (2007), Flow patterns in compound channels with vegetated floodplains, *J. Hydraul. Eng.*, *133* (2), 148–159.

A. S. Antonarakis, Department of Organismic and Evolutionary Biology, Harvard University, 26 Oxford St., Cambridge, MA 02138, USA. (aantonarakis@oeb.harvard.edu)

J. Brasington, Institute of Geography and Earth Sciences, University of Wales, Llandinam Building, Penglais Campus, Aberystwyth, SY23 3DB, UK.

E. Muller, Laboratoire Dynamique de la Biodiversité, CNRS, 29 Rue Jeanne Marvig, 31055, Toulouse, France.

K. S. Richards, Department of Geography, University of Cambridge, Downing Place, Cambridge CB2 3EN, UK.